Infrared and far-infrared studies of zinc-compensated β-gallates

H. G. LeDuc* and L. B. Coleman
Department of Physics, University of California at Davis, Davis, California 95616

G. V. Chandrashekhar
IBM Thomas J. Watson Research Center, P.O. Box 218, Yorktown Heights, New York 10598

(Received 4 June 1984)

Single crystals of the fast-ion conductors M—β-gallate, where M is K, Rb, Ag, or Tl, have been prepared with small amounts of zinc. The zinc doping removes the excess oxygen ions usually found in the conduction plane. Infrared and far-infrared (6—4000 cm^{-1}) reflectance and transmission spectroscopy have been used to study the lattice dynamics of the zinc-doped spinel blocks and the conducting cations in the more open conduction plane. Comparing these spectra with the infrared and Raman spectra of the undoped and the stoichiometric gallates, we find that the occupation of sites in the conduction plane is different from that of the undoped materials. In addition, the conduction plane in the Tl—Zn—β-gallate is sufficiently disordered to violate the exclusion principle. No systematic changes were seen in the spinel block lattice modes with the addition of the zinc or the increased cation density which results.

I. INTRODUCTION

Some of the most extensively studied of the fast-ion (or "superionic") conductors have been the members of the β-alumina family. This interest has been sustained due to the availability of a wide range of conduction ion species, at least three distinct levels of stoichiometry, and the two dimensionality of the conduction mechanism, as well as possible technological applications for energy production and storage.[1] We have studied the infrared and far-infrared response of several members of the β-gallate family of fast-ion conductors. The gallates are the gallium isomorphs of the β-aluminas. The "ideal" formula unit for these compounds is $M_2O{\cdot}11Ga_2O_3$ with M being a monovalent metal. In practice, however, this stoichiometry is difficult to achieve and there is usually an excess of cations. In the potassium salt, for example, the stoichiometric material would contain two K^+ ions per cell similar to the β-alumina. However as typically prepared K—β-gallate contains 2.72 K ions with the excess charge compensated by extra O^{2-} ions in the conduction plane. The crystal structure of these materials has been described in detail.[2] The mobile ions reside in sites in the a-b plane separated from each other by "spinel blocks" formed from Ga_2O_3 units stacked along the c axis. The spinel blocks are bound to each other by bridging oxygen ions (O^{2-}) which reside in the conduction plane. There are several sites available to the conducting cations referred to as the Beevers-Ross (BR), the anti-Beevers-Ross (aBR), and the midoxygen (mO) sites. The Beevers-Ross site is favored in the stoichiometric material; however, nonstoichiometry is found to alter the site preferences depending on the properties of the cation (particularly ionic size and polarizability) and the mode of charge compensation.

The mechanism of charge compensation in the gallates has been found to vary with the method of sample preparation and the mobile-ion species. This phenomenon is important since the charge compensation mechanism has a large effect on the concentration of mobile ions and the nature of the charge carrier transport. For example, in the potassium gallate system there are at least three distinctly different methods of charge compensation.[3] (1) In the material obtained by ion exchange of K^+ for the mobile Na ion of as-grown Na—β-gallates, the charge of the approximately 45 at. % excess alkali is compensated in part by interstitial oxygens and in part by the effective double-negative charge on Na^+ substituted for a Ga^{3+} ion in the spinel block.[4] (2) In the compound obtained directly from $K_2O{\cdot}2Ga_2O_3$ melts by slow vaporization of K_2O, the approximately 36 at. % excess K^+ is compensated entirely by interstitial O^{2-} ions.[3] (3) In the material obtained directly from $ZnO{\cdot}K_2O{\cdot}Ga_2O_3$ melts by K_2O vaporization, the nearly 67 at. % excess K^+ is compensated entirely by the effective negative charge on the Zn^{2+} substituting for Ga^{3+} in the spinel block. Ion-exchanged solids usually inherit the charge-compensation mechanism of the parent compound, especially if that mechanism involves defects in the spinel blocks, as diffusion in these covalently bonded structures is limited. Thus, the method of preparation is important. For example, K—β-gallate as-grown (mechanism 2) and that obtained from ion exchange of Na—β-gallate (mechanism 1) will exhibit a number of different properties. Therefore it is important to completely specify the methods of preparation used when describing the samples under study.

We have completed an infrared and far-infrared study of the vibrational modes of a series of gallate single crystals belonging to the third group described above; the as-grown K—Zn—β-gallate, and Ag, Tl, and Rb—Zn—β-gallates obtained by ion exchange of the K—Zn—β-gallate crystals. In these gallates, the effect of zinc doping is the same as that of Mg^{2+} doping in Mg-doped β''-alumina. Zn^{2+} substitutes for Ga^{3+} in the spinel block and ac-

counts for all of the charge compensation,[3] leaving the conduction plane free of excess oxygen ions. This results in not only a "cleaner" conduction plane, but also in an even larger concentration of mobile ions, 3.36 mobile ions per cell versus 2 for the ideal stoichiometric material and 2.72 for the typical oxygen-compensated materials. This is the highest alkali content of any β-phase fast-ion conductor. However, the removal of the excess O^{2-} ions from the conduction plane in the potassium salt results in a negligible decrease in the activation energy (0.245 versus 0.25 eV) and only a small increase in the ionic conductivity below 600 K.[3]

The infrared and Raman responses of aluminates and gallates have been extensively studied;[1,5–8] however, this is the first infrared study of the zinc-doped compounds M—Zn—β-gallate (M denotes Ag, Tl, and Rb; K—Zn—β-gallate has been investigated by Burns and coworkers,[9] who have also completed Raman studies of the zinc-doped compounds[10]). Optical studies of undoped gallates and aluminates show that the weak binding between the spinel blocks and conduction ions lead to spectra in which the spinel modes (in the spectral region above 200 cm^{-1}) are largely unaffected by the choice of conduction cation. Modes involving motion of the conducting ion (observed below 200 cm^{-1}) are sensitive to details of the crystal environment and chemistry, including the degree of nonstoichiometry, the method of charge compensation, and the occupancy of the available sites (which depends on M, as noted above). The primary interest of this study was to determine the effects of the zinc centers and the removal of excess oxygen ions from the conduction plane on the vibrational spectra and dynamics of the mobile ions.

II. EXPERIMENTAL DETAILS

Single crystals of K—Zn—β-gallates were grown by slow vaporization of $K_2O{\cdot}2Ga_2O_3$ melts with added ZnO.[3,11] The addition of 4% or more ZnO to the melt results in a constant level of approximately 5 at. % zinc in the crystal, corresponding to a composition of $1.67K_2O{\cdot}1.33ZnO{\cdot}10.34Ga_2O_3$, where all of the potassium and none of the zinc are mobile. Crystals of Ag, Rb, and Tl—Zn—β-gallates were prepared by ion-exchanging all of the K^+ ions in the K—Zn—β-gallate crystals with Ag^+, Rb^+, or Tl^+ in $AgNO_3$, $RbNO_3$, or $TlNO_3$ melts. The easy cleavage of the a-b plane produced crystalline faces which required no further polishing for use in the infrared and far-infrared.

Unpolarized (E field parallel to the a-b plane) reflectance and transmission spectra were measured at room temperature and at near-normal incidence in the range 6–4000 cm^{-1}. In the far-infrared (6–400 cm^{-1}), a modified Beckman FS 720 Michelson interferometer was used. The interferometer is controlled by a Digital Equipment Corporation PDP 11/23 minicomputer, which is also used for real-time data acquisition and Fourier transform analysis. Two gallium-doped germanium composite bolometers[12] were used, one optimized for low frequency and low background radiation was operated at 1.7 K, and the other, optimized for higher-frequency use, was operated at 4.2 K. A combination of scatter and transmission low-pass filters are mounted in the detector cryostat and cooled to either 1.7 or 4.2 K. Standard phase-sensitive detection techniques were used with an ultralow-noise preamplifier and lock-in amplifier input to an analog-to-digital converter. Additional noise reduction and spectral averaging as well as Fourier transformation and normalization were carried out in software. In the infrared from 250 to 4000 cm^{-1}, a Nicolet MX-1E Fourier transform infrared (FTIR) spectrometer was used. This instrument uses a cesium-iodide beamsplitter and a room-temperature TGS (triglycine sulphate) detector. Both spectrometers were used with locally constructed reflectance apparatus designed for near-normal incidence. Special care was taken to stop the stray light reflected from the sample holder or transmitted by the sample from reaching the exit optics. Polished brass mirrors machined to match the sample dimensions were used to obtain the instrument background reflectance spectra. Absolute transmission was measured by masking the beam to match the sample size. Data were taken with a resolution of 1 cm^{-1} in the infrared (analysis was performed on spectra with resolution reduced to 2 cm^{-1}), 2 cm^{-1} in the far-infrared (50–300 cm^{-1}), and 0.45 cm^{-1} below 50 cm^{-1}. Details of the experimental apparatus and sample-preparation techniques can be found elsewhere.[13]

III. RESULTS

The room-temperature reflectivity of the K, Rb, Ag, Tl, and Ag—Zn—β-gallates are shown in Fig. 1. The reflectivity was measured to above 4000 cm^{-1}; however, it remains small and featureless above 800 cm^{-1}. The transmission spectra produced the same information as the reflectance results and were used only as a check of the low-frequency (6–20 cm^{-1}) analysis as discussed below. We model the optical response of these materials using a sum of classical damped harmonic oscillators (Lorentzian modes). The frequency-dependent complex dielectric function (the response function responsible for the measured spectra) is then written as

$$\tilde{\epsilon}(\omega)=\epsilon_\infty+\sum_j \frac{f_j\omega_{0j}^2}{\omega^2-\omega_{0j}^2-i\gamma_j\omega}\ , \tag{1}$$

where ϵ_∞ is the electronic part of the dielectric constant, f_j is the oscillator strength,[14] ω_{0j} is the transverse optical mode frequency, and γ_j is the damping coefficient.

The real and imaginary parts of the dielectric function are then given by

$$\epsilon_1=\epsilon_\infty+\sum_j \frac{S_j(\omega^2-\omega_{0j}^2)}{(\omega^2-\omega_{0j}^2)^2+\gamma_j^2\omega^2}\ , \tag{2}$$

$$\epsilon_2=\sum_j \frac{S_j\gamma_j\omega}{(\omega^2-\omega_{0j}^2)^2+\gamma_j^2\omega^2}\ , \tag{3}$$

and the imaginary part of the dielectric constant is related to the real part of the conductivity as

$$\sigma_1(\omega)=\frac{\omega\epsilon_2(\omega)}{4\pi}\ . \tag{4}$$

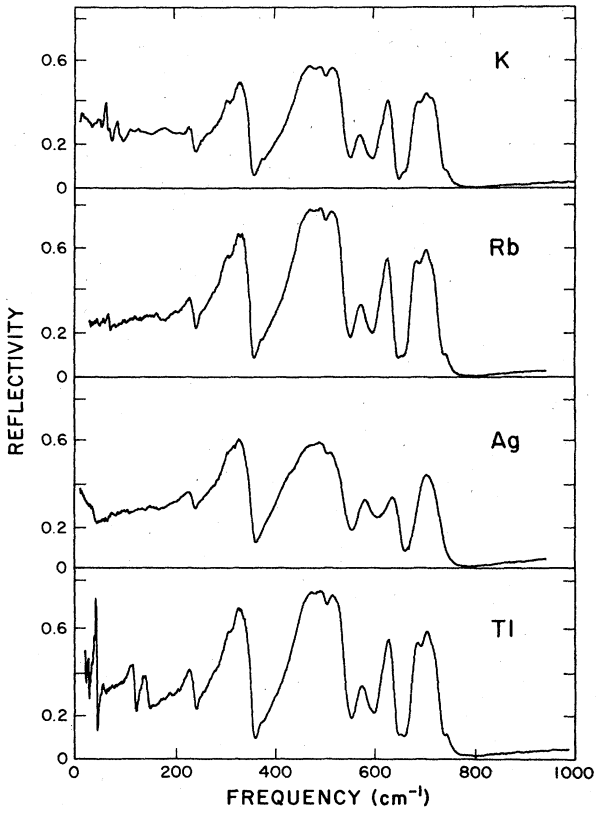

FIG. 1. Infrared and far-infrared reflectivity of single crystals of M—Zn—β-gallate with M = K, Rb, Ag, and Tl.

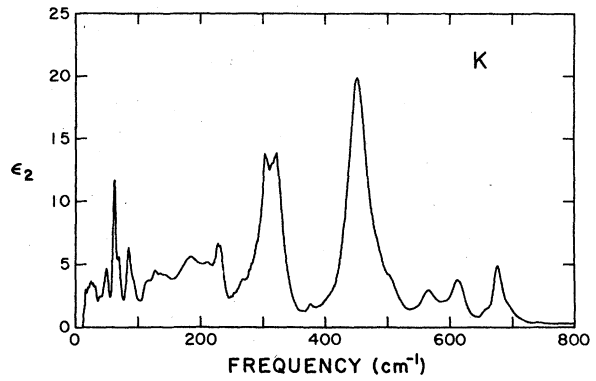

FIG. 2. Imaginary part of the room-temperature dielectric function [$\epsilon_2(\omega)$] of K—Zn—β-gallate determined by Kramers-Kronig analysis, vs frequency.

The dielectric function is more easily visually interpreted than the reflectance. For small damping the peaks of $\epsilon_2(\omega)$ occur at the transverse optical mode frequencies. The width of the modes at half maximum is the damping or inverse lifetime. The peaks in the imaginary part of the inverse dielectric function, $\mathrm{Im}(-1/\tilde{\epsilon})$, occur at the longitudinal normal mode frequencies. The oscillator strength is proportional, via the sum rules, to the integrated conductivity. When damping becomes significant, more care must be taken in obtaining the mode frequencies.

The complex dielectric function was obtained from the measured reflectance using a Kramers-Kronig analysis.

TABLE I. Normal-mode parameters for M—Zn—β-gallates. ϵ_∞, ω_{t0}, γ, and f as defined in Eq. (1); ω_{t0} and γ in cm^{-1}.

K			Rb			Ag			Tl		
ω_{t0}	γ	f	ω_{t0}	γ	f	ω_{t0}	γ	f	ω_{t0}	γ	f
28	25	3.06							21	2.2	0.91
49	7	0.50	(45)[a]			34	15	1.73	23	2	1.32
61	5	8.73							31	2	0.31
69	8	4.2	67	4.5	0.19				36	3	2.47
84	8	0.43							38	1.2	1.39
93	15	0.38									
114	13	0.29							111	8	1.14
128	15	0.46	165	20	0.28				137	16	1.28
229	15	0.40	232	10	0.41	229	15	0.36	228	12	0.67
267	24	0.22									
304	20	0.70	305	12	1.07	306	24	1.92	304	18	1.73
322	20	0.66	320	15	1.66	321	20	0.92	317	15	1.19
452	36	0.57	448	23	2.69	448	55	2.19	448	22	2.39
503	25	0.11	504	12	0.02	505	18	0.22	505	16	0.02
565	37	0.14	565	28	0.14	572	36	0.20	565	28	0.16
612	23	0.12	610	16	0.18	624	28	0.15	613	14	0.17
659	15	0.12	654	12	0.01				652	12	0.012
677	15	0.10	673	15	0.12				672	15	0.12
			694	12	0.007	684	25	0.14	694	12	0.008
			740	15	0.004				740	15	0.004
$\epsilon_\infty = 3.61$			$\epsilon_\infty = 3.68$			$\epsilon_\infty = 3.59$			$\epsilon_\infty = 3.65$		

[a] Channel spectra obscured peak.

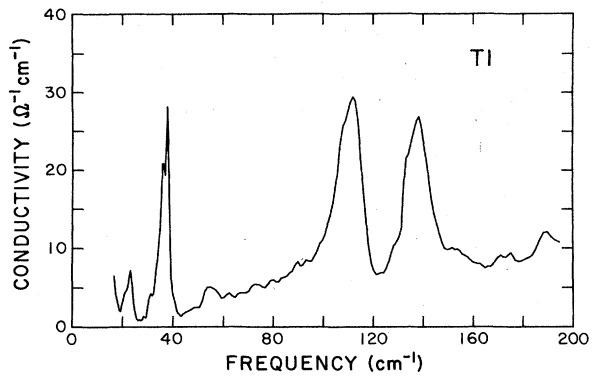

FIG. 3. Far-infrared conductivity of Tl—Zn—β-gallate determined by Kramers-Kronig analysis, vs frequency.

This technique allows for the calculation of the frequency-dependent complex dielectric function from a knowledge of the reflectivity over all frequencies. Extrapolations are made for frequencies outside of the experimentally measured range.[15] At high frequency, free-electron behavior is simulated, and our low-frequency extrapolations were chosen to agree with the transmission spectra which extend to a frequency lower than the reflectance measurements. Experience has shown that when the data extend over several decades or more in frequency, and care is taken in the extrapolations, the Kramers-Kronig techniques give reliable and reproducible results. Examples of the results of this procedure are shown in Figs. 2 and 3.

The normal mode parameters (frequency, width, and oscillator strength) were obtained by fitting the imaginary part of the dielectric function to the Lorentzian oscillator model [Eq. (3)] and then fitting the reflectance directly. This procedure has been found to be easier than a direct fit to the reflectance because of the more direct interpretation of the fitting parameters in terms of structures in the imaginary part of the dielectric function. The fits are performed in an interactive computer routine with visual comparisons of the data and the calculated results. Fitting directly to the reflectance in the final stages effectively eliminates any deleterious effects of the extrapolations used in the Kramers-Kronig transformation. Table I contains the mode parameters from the final fits to the reflectance spectra.

IV. DISCUSSION

Examination of the spectra of the undoped (prepared from as-grown Na—β-gallate) and zinc-doped M—β-gallates reveals a wealth of structure. The space group of the ordered β-gallates is $P6_3/mmc$ (D^4_{6h}), and group-theoretic analysis[8,16,17] yields 27 infrared-active modes (15 E_{1u} and 12 A_{2u}). A_{2u}-symmetry modes involve motions perpendicular to the conducting plane (i.e., along the c axis) and are inaccessible to us. Of the 15 E_{1u} modes, 13 involve the atoms in the spinel blocks and the remaining two E_{1u} modes arise from the cations at the BR sites (in the ordered material, the only occupied sites). The observed spectra are consistent with those of the other members of the aluminate-gallate family. Above 200 cm^{-1} there is nearly a one-to-one correspondence between the lattice mode parameters, independent of the conducting species, and we therefore assign these modes to vibrations of the spinel blocks. The infrared and Raman spectra of β-Ga_2O_3 (pure gallate) and stoichiometric sodium β-gallate have been calculated as well as measured by Dohy and co-workers.[18,19] The correspondence between many of these modes adds further support to the assignment of the high-frequency modes to the spinel blocks. The thallium, potassium, and rubidium samples studied here are nearly identical in this region, while the silver sample exhibits minor differences above 500 cm^{-1} in both frequency and line shape. These latter variations may not represent true differences in the bulk properties as the silver crystals were of poorer quality, with rougher surfaces and dark inclusions in the bulk.

Comparing the spectra of the zinc-doped (prepared from K—Zn—β-gallate) and undoped gallates (prepared from Na—β-gallate), we find no systematic changes in the spinel block modes, suggesting that the increased cation density, removal of excess bridging oxygen, and the addition of a low density (4%) of zinc defect centers have no significant effect on the spinel-block lattice dynamics. In addition, the zinc centers do not disorder the gallate lattice sufficiently to cause a breakdown of the Raman and infrared selection rules (as discussed further below).

In these materials the spectra at low frequency (below 200 cm^{-1}) depend strongly on the type of mobile cation and the level of stoichiometry. The complexity of the spectra is a function of the number and types of occupied sites and the interactions internal to complexes of cations, as well as between the cations and the spinel blocks. In particular, in the zinc-doped β-gallates we expect the following.

(1) The increased cation density will result in additional structure from the increased site occupancies;

(2) New features arising from the interactions between cations in the more open and cation-rich conduction plane (M-M complexes);

(3) Interactions between the cations and the negative zinc defects in the spinel blocks (M-Zn complexes);

(4) A reduction or disappearance of the structure arising from interactions between the cations and the excess oxygen ions in the conduction plane (M-O complexes); and

(5) A reduction in the modes of the Ga—O—Ga bridges between the spinel blocks.

It is well known that in the aluminas the relative occupancies of the three major cation sites in the conduction plane (BR, aBR, and mO) vary greatly from cation to cation. For example, in K—β-alumina the percentages are 54:0:46 (BR:aBR:mO) versus 70:30:0 in Tl—β-alumina.[2] Variations in the relative occupancy rates are also seen as the stoichiometry is varied.[4,20] While the same wealth of crystallographic data that exists on the aluminas does not as yet exist for the gallates and the zinc-doped gallates, we assume that the site-occupancy levels are equally sensitive to cation species and stoichiometry. By combining our results with the existing crystallographic data and infrared and Raman spectra for the aluminas, undoped gallates,

and stoichiometric gallates, we can propose some mode assignments. In stoichiometric materials the cations will occupy the BR sites. Colomban and Lucazeau,[21] in their studies of the stoichiometric β-gallates, assign the modes at 84 cm^{-1} (K), 35 cm^{-1} (Ag), and 37 cm^{-1} (Tl) to the in-plane cation oscillations at the Beevers-Ross site. Thus we can assign the 84.5 cm^{-1} (K), 34 cm^{-1} (Ag), and 36,38 cm^{-1} (Tl) modes to the in-plane vibrations of the cations on the BR sites in the zinc-doped gallates. The Rb—Zn—β-gallate sample displayed channel spectra at low frequencies, making analysis difficult; however, there is evidence in the reflectance spectra of a mode at 45 cm^{-1}. (The transmittance confirms this as it drops to zero there.) However, we cannot assign this mode to cation oscillations in a particular site due to the lack of site-occupancy data or spectra of the stoichiometric material. We have been unable to determine the cause of the splitting of the 37 cm^{-1} mode in thallium gallate into the 36,38 cm^{-1} pair in the zinc-doped material.[22] It is most likely caused by some type of cation complexing in the conduction plane; however, without detailed normal-mode analysis and x-ray crystallographic studies it is not possible to explain this splitting or to make assignments of the remaining low-frequency modes.

Colomban and Lucazeau[21] have assigned the modes near 100 cm^{-1} to the Ga—O—Ga bridges in the stoichiometric β-gallates. Of these assigned modes we observe only the modes at 111 and 137 cm^{-1} in Tl—Zn—β-gallate. These frequencies are 3 to 4 cm^{-1} lower than those proposed by Colomban and Lucazeau for the stoichiometric gallate, and 2 and 7 cm^{-1} below those seen by Burns[7] in the undoped material derived from Na—β-gallate. In those materials where the undoped spectra have been studied [Tl and K (Ref. 7)], no major changes in the intensity of these modes was seen, as the doping removed excess oxygen bridges.

Burns and co-workers have explored the Raman spectra of the undoped[8] and zinc-doped[10] β-gallates (Table II). Since the ideal structure of these materials has a center of inversion, eigenvectors of each irreducible representation have definite parity, as do the Raman and infrared operators. Thus the exclusion rule (in which Raman and infrared modes must transform by different irreducible representations) is in effect and the mode frequencies should be unique (except for accidental degeneracy). Cation disorder in the conduction plane can lead to a breakdown of the inversion symmetry, and thus it is possible for Raman and infrared modes to be degenerate. Burns *et al.*[8] found that the exclusion rule is indeed broken for the low-frequency cation modes in the β-aluminas, but that it is still valid in the undoped β-gallates. However, the increased cation density in the zinc-doped Tl—β-gallate may have created sufficient disorder to violate the exclusion principle. The 21, 23, and 31 cm^{-1} modes we have observed in Tl—Zn—β-gallate may correspond to the Raman modes at 21 and 35 cm^{-1} in Tl-Zn gallates and those at 20 and 32 cm^{-1} in the undoped gallates. The appearance of a mode at 37 cm^{-1} in the Raman spectra upon going from thallium to thallium-zinc (possibly corresponding to the 36,38 cm^{-1} mode in our infrared data) adds strength to this interpretation. In the ordered conduction plane of the stoichiometric gallates and aluminates, no breakdown of selection rules is seen.[21] We cannot totally rule out accidental degeneracy in the thallium gallate since the same effect is not observed in the potassium, silver, or rubidium materials. However, from a consideration of the frequency differences between in-plane modes of different symmetry, Colomban and Lucazeau[21] have shown that the stoichiometric thallium compounds have strong interplane coupling. This would lead to a more significant loss of inversion symmetry, and therefore a violation of the exclusion principle in the thallium gallates. The weak coupling of the disordered cations to the spinel modes effectively makes inversion a good symmetry for the spinel modes, and no relaxation of the selection rules is seen at higher frequencies, as expected.

In summary, we find that the addition of zinc to charge-compensate the β-gallates allows for a redistribution of the cations in the conduction plane. In the potassium and thallium materials, where we can compare directly with the undoped gallates (prepared from Na—β-gallate), we find many more vibrational modes at low frequency, indicating a more varied distribution. The additional cation density does not appear to affect the structure and lattice dynamics of the spinel blocks. Unfortunately, without a complete crystallographic determination of the site occupancies and a normal mode analysis, we are unable to further explore the effects of the increased cation density and the more open conduction plane on the ionic conduction process.

TABLE II. Raman-mode frequencies of Zn-doped β-gallates (frequency in cm^{-1}). Data are the unpublished results of Burns (Ref. 10).

Rb—Zn—β-gallate	Tl—Zn—β-gallate	Ag—Zn—β-gallate
	21.0	
	35.07	
	37.2	
51.6	50.4	
58.6	56.0	62.9
72.0	70.04	
75.4	91.3	
	105.4	
175.8	176.1	172.0
	183.9	
205.2	212.5	209.6
263.0	256.0	
313.0	314.0	315.0
	341.0	
	355.0	
406.0	386.0	
434.7	427.1	428.5
501.4	497.3	502.4
	607.5	
656.2	656.2	654.0
676.3	673.8	671.0
		681.0
724.2	726.2	725.0

ACKNOWLEDGMENTS

We would like to thank Dr. Gerald Burns for helpful discussions and for the Raman scattering results of the zinc-doped materials. This work was a portion of the doctoral dissertation of one of us (H.G.L.).

---

*Present address: Jet Propulsion Laboratory, Pasadena, CA 91103.

[1]For a review of the field, see *Fast Ion Transport in Solids,* edited by J. B. Bates and G. C. Farrington (North-Holland, New York, 1981); S. Chandra, *Superionic Solids* (North-Holland, New York, 1981).

[2]J. H. Kennedy, in *Solid Electrolytes,* Vol. 21 of *Topics in Applied Physics,* edited by S. Geller (Springer, New York, 1977), p. 21.

[3]G. V. Chandrashekhar, L. M. Foster, and G. Burns, Solid State Ionics **5**, 175 (1981).

[4]M. P. Anderson, L. M. Foster, and S. J. La Placa, Solid State Ionics **5**, 211 (1981).

[5]For a recent review of the ir, Raman, and neutron-scattering results in the aluminas, see C. Lucazeau, Solid State Ionics **8**, 1 (1983), and references therein.

[6]S. J. Allen, Jr., A. S. Cooper, F. DeRosa, J. P. Remeika, and S. K. Ulasi, Phys. Rev. B **17**, 4031 (1978).

[7]H. R. Chandrashekhar, G. Burns, and G. V. Chandrashekhar, Solid State Commun. **27**, 829 (1978).

[8]Gerald Burns, G. V. Chandrashekhar, F. H. Dacol, L. M. Foster, and H. R. Chandrashekhar, Phys. Rev. B **22**, 1073 (1980).

[9]Gerald Burns, T. N. Theis, G. V. Chandrashekhar, and F. H. Dacol, Phys. Rev. B **26**, 3309 (1982).

[10]Gerald Burns (private communication). The samples used in the present work are the same crystals as investigated by Burns.

[11]G. V. Chandrashekhar and L. M. Foster, Solid State Commun. **41**, 701 (1982).

[12]N. S. Nishioka, P. L. Richards, and D. P. Woody, Appl. Opt. **17**, 1562 (1978).

[13]H. G. LeDuc, doctoral dissertation, University of California at Davis, 1983.

[14]It should be noted that the oscillator strength is written in several ways, usually as a dimensionless number (f) or in units of frequency squared (S). The two forms are related as $S_j = f_j \omega_{0j}^2$.

[15]For a discussion of Kramers-Kronig techniques, and extrapolations to high and low frequency, see Fredrick Wooten, *Optical Properties of Solids* (Academic, New York, 1972).

[16]J. B. Bates and Roger Frech, Chem. Phys. Lett. **60**, 95 (1978).

[17]There is some apparent disagreement in the literature as to the number of modes expected. This is resolved when careful attention is taken as to whether or not the two cations are included in the analysis.

[18]D. Dohy, G. Lucazeau, and A. Revcolevschi, J. Solid State Chem. **45**, 180 (1982).

[19]D. Dohy, G. Lucazeau, and D. Bougeard, Solid State Ionics **11**, 1 (1983).

[20]J. M. Newsam and B. C. Tofield, Solid State Ionics **5**, 59 (1981).

[21]Ph. Colomban and G. Lucazeau, J. Chem. Phys. **72**, 1213 (1980).

[22]The resolution of the Tl—β-gallate spectra in Ref. 8 is not given; therefore the possibility remains that the mode reported at 37 cm^{-1} is an unresolved pair.